Low-field magnetic resonance imaging of changes after femoral osteosynthesis failure: a case report

J. Glodek*, Z. Adamiak, M. Mieszkowska, A. Przeworski

Faculty of Veterinary Medicine, University of Warmia and Mazury in Olsztyn, Olsztyn, Poland

*Corresponding author: j_glodek@wp.pl

ABSTRACT: We describe here a case study of a 16-month-old female European shorthair cat examined about 6 months after the osteosynthesis of a femoral fracture. Clinical examination revealed a non-weightbearing left limb, pain upon manipulation of the hip joint, complete immobilisation of the stifle joint and muscle atrophy in the left thigh. Low-field magnetic resonance images were acquired in sagittal, transverse and dorsal planes with T1-weighted spin echo, T2-weighted fast spin echo, T1-weighted gradient echo, gradient echo short tau inversion recovery and T1-weighted XBone sequences. Total examination time was 59 min 20 s. The obtained images revealed the presence of osteophytes on the surface of the femoral head, subluxation of the hip joint, atrophy and fatty infiltration of the quadriceps femoris muscle. The symmetry and size of callus in the fracture site were also evaluated. Based on the results of the magnetic resonance imaging exam, the patient was diagnosed with hip osteoarthritis, atrophy and fatty degeneration of the quadriceps femoris muscle with homogeneous and symmetrical distribution of callus in the fracture site. The results of this study confirm the high diagnostic value of low-field magnetic resonance imaging in diagnostics of musculoskeletal injuries in cats.

Keywords: feline; osteoarthritis; hip; muscle atrophy; fatty degeneration; callus

Computed tomography (CT) and magnetic resonance imaging (MRI) are popular three-dimensional imaging modalities, which allow the visualisation of internal anatomy without superimposition of adjacent structures. In human medicine, MRI is most frequently used to examine the central nervous system and the musculoskeletal system (Baird et al. 1998). The main advantages of MRI include multiplane imaging and good contrast between bone and the surrounding soft tissues (Zhalniarovich et al. 2014). MRI enables diagnosis of acute muscle injuries (muscle strain, laceration), acute complications (acute compartment syndrome, haematoma, fibrosis) and chronic dysfunctions (chronic compartment syndrome, muscle denervation, myositis ossificans, muscle herniation) as stated by Elsayes et al. (2006). MRI is used to determine the aetiology of disease (trauma, tumours, neuropathy, thrombi) and its progression (Kamath et al. 2008). The main disadvantages of this imaging method are the time and costs, which are higher compared to computed tomography. However, the dose of ionising radiation generated by a CT scanner is much higher than that emitted by an X-ray machine, and in this respect, MRI has a considerable advantage over CT. Thus, when both imaging modalities are available, MRI should be the method of choice.

The pathological processes most frequently observed in the feline hip joint include dysplasia, osteoarthritis and joint luxation (Grierson 2012; Glodek et al. 2015). Osteoarthritis occurs frequently in cats, but it is rarely diagnosed (Clarke et al. 2005; Lascelles 2010; Guillot et al. 2013). Degenerative changes are most often observed in elbow joints, followed by hip and stifle joints (Guillot et al. 2012). Joint and bone injuries are often accompanied by damage to the surrounding soft tissues. This article evaluates the usefulness of low-field MRI in diagnosing post-traumatic injuries in the feline musculoskeletal system.

Case description

The study was performed in a 16-month-old, sterilised female European shorthair cat with a body weight of 4.2 kg. The history of the animal was not clear, because of an absence of medical documents and the lack of contact with previous owners. Based on a clinical interview with shelter workers we suspected that the cat was injured about six months before the study. The injury was manifested as a simple transverse fracture of the mid-femoral shaft.

The animal was admitted to the clinic with a non-weightbearing left hind-limb. A clinical examination confirmed the presence of superficial and deep sensation, even distribution of temperature in both pelvic limbs and pronounced asymmetry of quadriceps femoris muscle mass. Pain upon manipulation of the hip joint, hyperextension and complete immobilisation of the stifle joint were also observed. A ventrodorsal radiograph (made using Gierth X-ray, Germany) of the left hip joint revealed flattening of the acetabulum with subluxation of the femoral head, abnormal shape of the femoral head, irregular surface of the femoral head, thickened femoral neck, skew of the bone long axis and the presence of callus (Figure 1). Based on the observed changes, a decision was made to examine the affected limb in a low-field MRI scanner (Vet Grande Esaote I, 0.25 T, Italy). The patient was anaesthetised prior to the examination to eliminate motion artefacts. Sedation was induced with intramuscular medetomidine administered at 0.05 mg/kg body weight (Cepetor 1 mg/ml, ScanVet, Poland). General anaesthesia was induced and maintained with intravenous bolus of propofol at 2 mg/kg body weight (*i.v.*; Scanofol 10 mg/ml, ScanVet, Poland). The cat was positioned in sternal recumbency with pelvic limbs extended caudally and hip joints positioned centrally in the knee coil (No. 2). The following sequences were applied in the dorsal plane: T1-weighted spin echo (SE T1, repetition time TR 470 ms, time echo TE 18 ms), T2-weighted fast spin echo (FSE T2, TR 3720 ms, TE 90 ms) and gradient echo short tau inversion recovery (GE STIR, TR 1370 ms, TE 25 ms). The sequences applied in the sagittal plane were T1-weighted spin echo (SE T1, TR 1150 ms, TE 26 ms), T2-weighted fast spin echo (FSE T2, TR 6580 ms, TE 120 ms) and T1-weighted gradient echo (GE T1, TR 830 ms, TE 16 ms). In the transverse plane, images were acquired in T1-weighted spin echo T1 (SE T1, TR 1350 ms, TE 26 ms), T2-weighted fast spin echo (FSE T2, TR 3200 ms, TE 90 ms) and XBone (TR 510 ms, TE 14; 28; 21; 21 ms) sequences. Slice thickness was 3 mm and slice gap was 0.3 mm for all sequences in sagittal and dorsal planes, and 2 mm and 0.2 mm in the transverse plane. Total examination time was 59 min 20 s, including the time required to perform the above protocol and the preceding scout and localiser sequences in dorsal, sagittal and transverse planes. T1-weighted SE in the sagittal plane was the longest sequence with a duration of 12 min.

RESULTS

The presence of osteophytes, defined as irregular foci with hypointense signals in SE T1 and FSE T2 sequences, was observed on the medial rim of the femoral head and the dorsal femoral neck (Figures 2 and 3). Images acquired with the use of the FSE T2 sequence in the sagittal plane revealed enlarged foci of hyperintense signal between the edge of the acetabulum and the femoral head, which are indicative of increased fluid accumulation inside
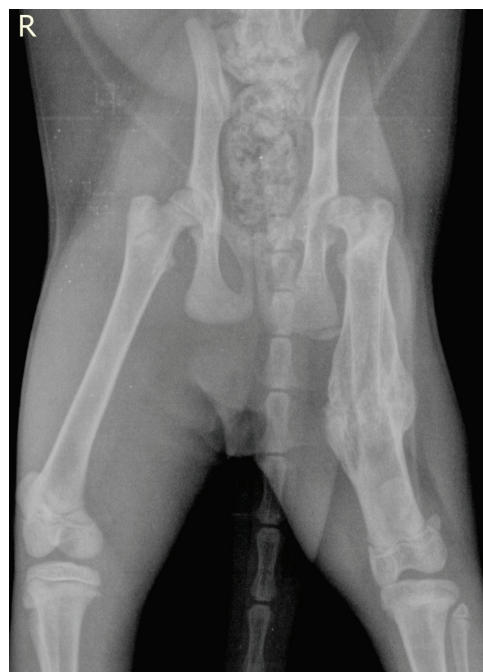

Figure 1. A ventrodorsal radiograph of the pelvis. Subluxation of the femoral head is accompanied by flattening of the acetabulum. The shape of the femoral head is abnormal and the surface of the femoral head is irregular. The femoral neck is thickened. Skewing of the bone long axis and the presence of a large callus are also observed
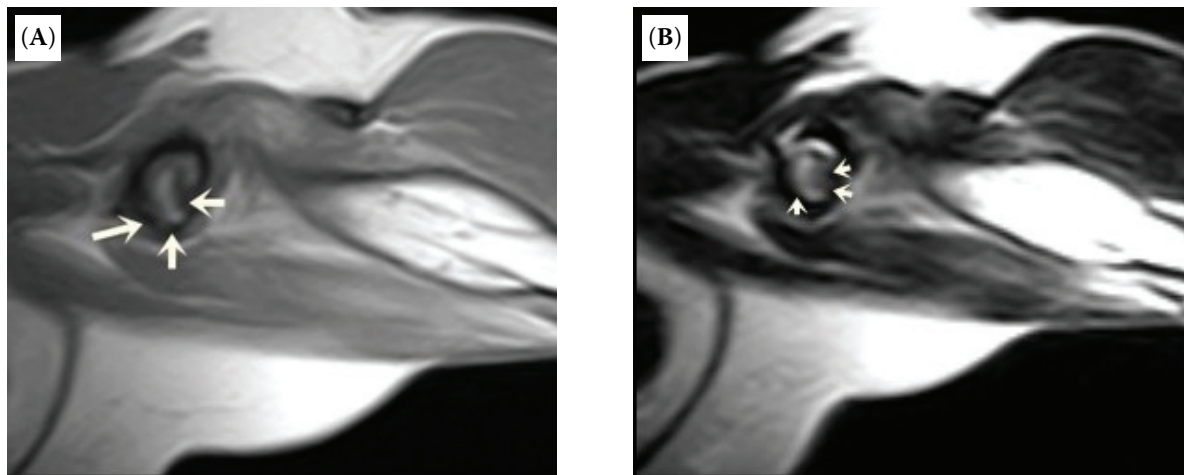
Figure 2. T1-weighted spin echo sequence in the sagittal plane (**A**) and T2-weighted fast spin echo sequence in the sagittal plane (**B**). The irregular focus of hypointense signal on the ventral surface of the femoral head on both sequences (white arrows) is indicative of osteophytosis

the joint (Figure 4). Flattening of the acetabulum and subluxation of the femoral head were visualised in the dorsal projection, which suggested the presence of osteoarthritis (Figure 5). Thigh muscles were characterised by varying signal intensity, with hyperintense signals in SE T1 and FSE T2 sequences (Figure 6) and hypointense signals in the STIR sequence in the region of the quadriceps femoris muscle. The observed changes in the signals in the above sequences were characteristic for fatty infil-
tration of muscle. Quadriceps muscle atrophy was clearly visualised. The fracture was stabilised by secondary healing and callus formation. The GE T1 sequence in the sagittal plane revealed a malunion of femoral bone and the presence of 12-mm-wide callus between fragments in the fracture site. In the transverse plane, calluses formed at the level of the fracture had a diameter of 12 mm and were characterised by uniform signal intensity (Figure 7). Based on the results of the MRI exam, the patient was diagnosed with left hip osteoarthritis, atrophy and fatty infiltration of quadriceps femoris muscle with homogeneous and symmetrical distribution of callus in the fracture site.
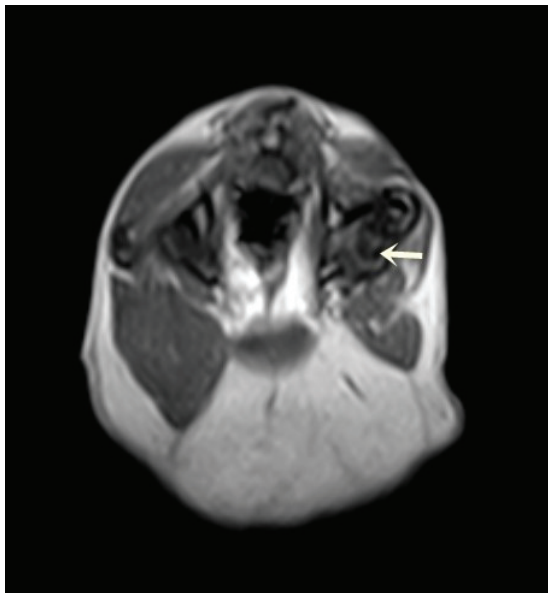

Figure 3. XBone sequence in the transverse plane (echo 2/4). The irregular focus of hypointense signal on the surface of the femoral head (white arrow) is indicative of osteophytosis
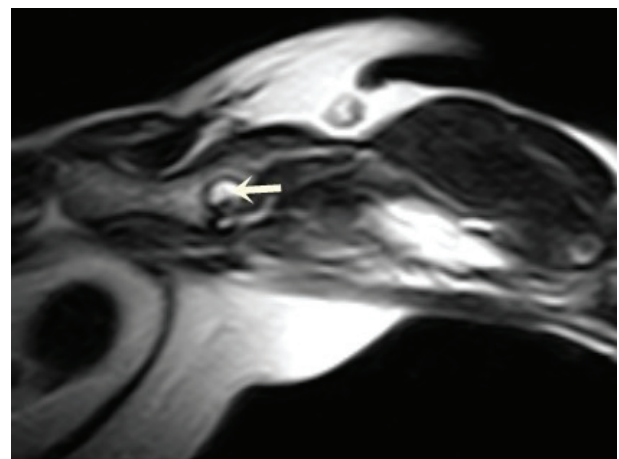

Figure 4. T2-weighted fast spin echo sequence in the sagittal plane. The area with a hyperintense signal from fluid (white arrow) is a sensitive indicator of increased synovial volume in the joint

Figure 5. T1-weighted spin echo sequence in dorsal plane. This plane corresponds to radiographic images in the ventrodorsal projection. The acetabulum (black arrows) is shallow and the shape of the femoral head (white arrow) is abnormal

Figure 6. T1-weighted spin echo sequence in the transverse plane (**A**) and T2-weighted fast spin echo sequence in the transverse plane (**B**). The hyperintense signals from the quadriceps femoris muscle on both sequences is indicative of fatty degeneration (white arrows). Atrophy of thigh muscles is also observed

DISCUSSION

Three imaging planes supported the spatial visualisation of the hip joint. Images acquired in the dorsal plane, which correspond to radiographic images in the ventrodorsal projection, enabled observations of joint symmetry, stability of the femoral head in the acetabulum and degenerative changes. Images acquired in the transverse plane were highly useful in localising changes, determining the degree of atrophy in thigh muscles and m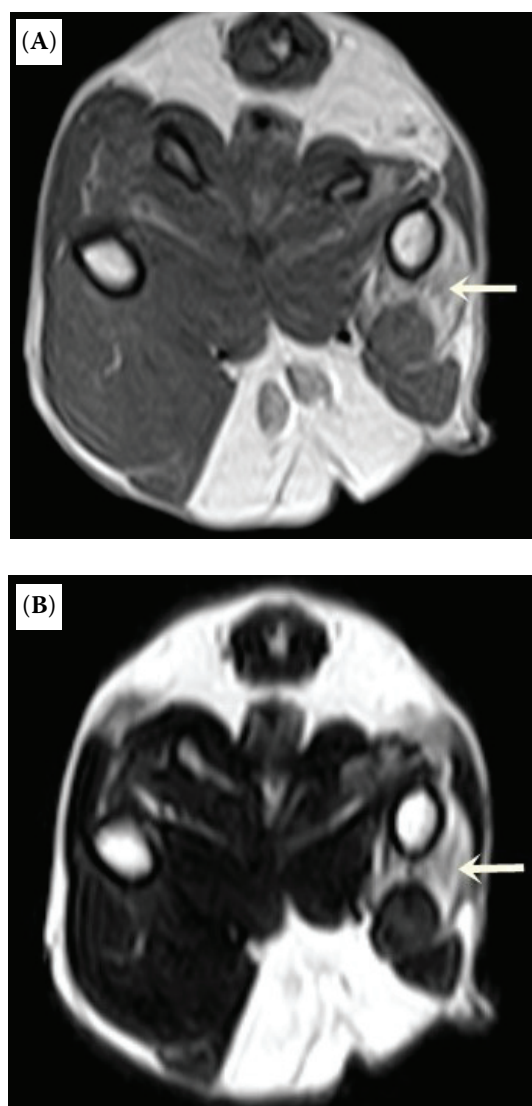easuring callus diameter. The sagittal plane corresponded to radiographic images in the "frog leg lateral view" and supported evaluations of hip joint subluxation, malunion of femoral bone and visualisation of muscles along their entire length.

Total examination time was 59 min and 20 s, which is similar to that reported by Guillot et al. (2012) in a high-field MRI (1.5 T) examination of feline hip joints (60 min). In both studies, examination time was twice as long as that reported by Kamishina et al. (2006) in a high-field MRI (4.7 T) scan. Those differences can be attributed to the fact that magnetic field strength significantly influences examination time.
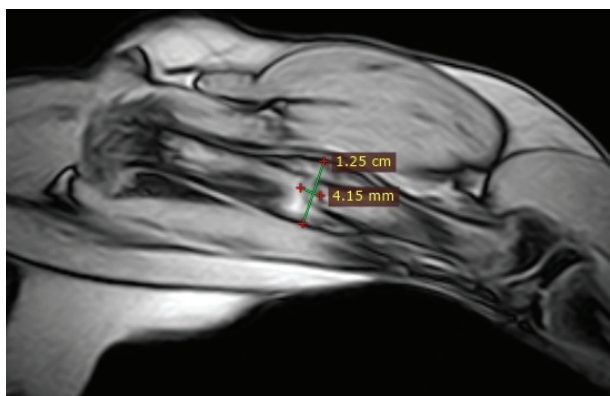
Figure 7. T1-weighted gradient echo sequence in the sagittal plane. Measurements of callus diameter and dislocation of bone fragments are indicated with lines

Feline joint osteoarthritis is most often accompanied by the presence of osteophytes or enthesophytes, sclerotisation, subluxation, chondromalacia with cysts and the formation of calluses (Lascelles et al. 2010). In a radiographic examination, the symptoms of feline joint osteoarthritis are similar to the changes observed in other animal species, but in cats, osteophyte formation usually affects the hip joint. Joint-associated mineralisation is significantly more prevalent in cats than dogs (Freire et al. 2011). Densification of the cancellous bone is observed at the insertion site of the ligament of the femoral head (Kamishina et al. 2006). In T1- and T2-weighted MRI sequences, such densification is visualised as a regular oval-shaped area with hypointense signal. However, it should not be over-interpreted as a degenerative change, which is also characterised by hypointense signal on the surface of the femoral head, as the latter is further characterised by an irregular shape. Changes of this type are also noted on the edge of the acetabulum and the femoral neck. In the examined patient, the presence of osteophytes and fluid accumulation in the left hip joint obtained with MRI scans corresponded with abnormalities on radiographic images (irregular surface and subluxation of the femoral head). These symptoms were indicative of inflammatory and degenerative processes. According to the literature, degenerative changes result from trauma in 25% of cases (Clarke et al. 2005). The presence of degenerative changes in joints caused by limb immobilisation was also determined experimentally (Jurvelin et al. 1986; Glodek et al. 2015).

Muscle atrophy and fatty degeneration are abnormalities which can be detected by computed tomography and MRI. The MRI examination of normal muscles revealed structures with moderate signal intensity, separated by hyperintense signals from adipose tissue in both T1- and T2-weighted images. In acute degenerative changes resulting from biochemical processes in muscles (decrease in protein levels, fatty infiltration), fat suppression and higher signal intensity are observed in T1-weighted images (Kamath et al. 2008). On CT images, the presence of streaks or low-density regions in muscles are indicative of fatty infiltration (Fuchs et al. 1999). The lesions with a fatty margin are easy to determine on CT; however, many pathological processes (for example, the presence of fibrous tissue) can be difficult to distinguish from the muscle tissue (Fuchs et al. 1999). In the discussed case, muscle atrophy was clearly visualised in the left pelvic limb. Higher signal intensity on the surface of the quadriceps femoris muscle in T1- and T2-weighted images and signal attenuation in the STIR sequence are indicative of fatty infiltration. In a study of rats performed eight weeks after musculus soleus injury, changes on the muscle surface were not detected in a T1-weighted sequence, but in a T2-weighted sequence, regenerated fibres were characterised by a minor increase in signal intensity relative to the surrounding healthy tissue (Winkler et al. 2011). In another study of rats performed 21 days after post-operative injury of multifidus muscles, hyperintense signals in a T2-weighted sequence may have been indicative of incomplete muscle regeneration due to nerve damage (Gejo et al. 2000). In the case described here the changes in the signals in T1 and T2- weighted sequences point to the chronic nature of the observed changes.

In the examined patient, the fracture was stabilised by secondary healing and callus formation. Those processes are stimulated by dynamic forces and movement of bone fragments. In the sagittal plane, the callus formed at the level of the fracture had a diameter of 12 mm. The measurements conducted in the transverse plane supported an evaluation of the symmetry of fracture healing, and the absence of changes in signal intensity was indicative of a normal healing process. MRI provides significant advantages over conventional radiography because it supports spatial visualisation of the healing process and eliminates errors resulting from limb rotation (Lujan et al. 2010). The GE T1 sequence was used to differentiate calluses from primary bone and to visualise the space

between bone fragments which was not present in the radiograph. The GE sequence is also efficient for visualisation of structures of tendons and ligaments (Adamiak et al. 2011).

The results of this study confirm the high diagnostic value of low-field MRI in examination of musculoskeletal injuries in cats. The applied sequences and planes supported evaluations of the hip joint, femoral fracture healing and muscle injuries. Comprehensive evaluations of bones and soft tissues in the musculoskeletal system contribute to accurate diagnoses.

REFERENCES

Adamiak Z, Jaskolska M, Matyjasik H, Pomianowski A, Kwiatkowska M (2011): Magnetic resonance imaging of selected limb joints in dogs. Polish Journal of Veterinary Sciences 14, 501–505.

Baird DK, Hathcock JT, Rumph PF, Kincaid SA, Visco D (1998): Low-field magnetic resonance imaging of the canine stifle joint: normal anatomy. Veterinary Radiology and Ultrasound 39, 87–97.

Clarke SP, Mellor D, Clements DN, Gemmill T, Farrell M, Carmichael S, Bennett D (2005): Prevalence of radiographic signs of degenerative joint disease in a hospital population of cats. Veterinary Record 157, 793–799.

Elsayes KM, Lammle M, Shariff A, Totty WG, Habib IF, Rubin DA (2006): Value of magnetic resonance imaging in muscle trauma. Current Problems in Diagnostic Radiology 35, 206–212.

Freire M, Robertson IAN, Bondell HD, Brown J, Hash J, Pease AP, Lascelles BDX (2011): Radiographic evaluation of feline appendicular degenerative joint disease vs. macroscopic appearance of articular cartilage. Veterinary Radiology and Ultrasound 52, 239–247.

Fuchs B, Weishaupt D, Zanetti M, Hodler J, Gerber C (1999): Fatty degeneration of the muscles of the rotator cuff: assessment by computed tomography versus magnetic resonance imaging. Journal of Shoulder and Elbow Surgery 8, 599–605.

Gejo R, Kawaguchi Y, Kondoh T, Tabuchi E, Matsui H, Torii K, Kimura T (2000): Magnetic resonance imaging and histologic evidence of postoperative back muscle injury in rats. Spine 25, 941–946.

Glodek J, Adamiak Z, Przyborowska P, Zhalniarovich Y (2015): Usefulness of magnetic resonance imaging in the diagnosis of feline hip joint disorders. Medycyna Weterynaryjna 71, 403–406.

Grierson J (2012): Hips, elbows and stifles. Common joint diseases in the cat. Journal of Feline Medicine and Surgery 14, 23–40.

Guillot M, Moreau M, d'Anjou MA, Martel-Pelletier J, Pelletier JP, Troncy E (2012): Evaluation of osteoarthritis in cats: Novel information from a pilot study. Veterinary Surgery 41, 328–335.

Guillot M, Moreau M, Heit M, Martel-Pelletier J, Pelletier JP, Troncy E (2013): Characterisation of osteoarthritis in cats and meloxicam efficacy using objective chronic pain evaluation tools. The Veterinary Journal 196, 360–367.

Jurvelin J, Kiviranta I, Tammi M, Helminen JH (1986): Softening of canine articular cartilage after immobilization of the knee joint. Clinical Orthopaedics and Related Research 207, 246–252.

Kamath S, Venkatanarasimha N, Walsh MA, Hughes PM (2008): MRI appearance of muscle denervation. Skeletal Radiology 37, 397–404.

Kamishina H, Miyabayashi T, Clemmons RM, Farese JP, Uhl EW, Silver X (2006): High Field (4,7 T) magnetic resonance imaging of feline hip joints. Journal of Veterinary Medical Science 68, 285–288.

Lascelles BDX (2010): Feline degenerative joint disease. Veterinary Surgery 39, 2–13.

Lascelles BDX, Henry III JB, Brown J, Robertson I, Sumrell AT, Simpson W, Pease A (2010): Cross-sectional study of the prevalence of radiographic degenerative joint disease in domesticated cats. Veterinary Surgery 39, 535–544.

Lujan TJ, Henderson CE, Madey SM, Fitzpatrick DC, Marsh JL, Bottlang M (2010): Locked plating of distal femur fractures leads to inconsistent and asymmetric callus formation. Journal of Orthopaedic Trauma 24, 156–162.

Winkler T, von Roth P, Matziolis G, Schumann MR, Hahn S, Strube P, Stoltenburg G, Perka C, Duda GN, Tohtz SV (2011): Time course of skeletal muscle regeneration after severe trauma: Muscle function against the background of MRI and histological findings. Acta Orthopaedica 82, 102–111.

Zhalniarovich Y, Adamiak Z, Glodek J, Przyborowska P, Holak P (2014): Comparison of High Resolution Gradient Echo, XBONE T1, XBONE T2, Spin Echo T1 and 3D SST1 magnetic resonance imaging sequences for imagining the canine elbow. Polish Journal of Veterinary Sciences 17, 587–591.